

A HIGHLY SENSITIVE CMOS-MEMS CAPACITIVE TACTILE SENSOR

Cheng-Ting Ko², Jhy-Ping Wu³, Wen-Chih Wang³, Ching-Hsiao Huang³, Sheng-Hsiang Tseng⁴,
Yung-Lin Chen⁴, and Michael S.-C. Lu^{1,2}

¹Department of Electrical Engineering and ²Institute of Electronics Engineering,
National Tsing Hua University, Hsinchu, Taiwan, R.O.C.

³Touch Micro-system Technology, Taoyuan Hsien, Taiwan, R.O.C.

⁴Chip Implementation Center, National Applied Research Laboratories, Hsinchu, Taiwan, R.O.C.

ABSTRACT

This paper describes the design and characterization of a capacitive tactile sensor fabricated in a conventional CMOS process. To achieve a high capacitive sensitivity, an oscillator circuit is adopted to convert the pressure induced capacitive change to an output frequency shift. The complete post micromachining steps are performed on a CMOS die without resorting to a wafer process. The pressure-sensing membrane has a total size of $200\ \mu\text{m} \times 200\ \mu\text{m}$ with an initial sensing capacitance of 153 fF. Experimental results show an initial frequency output at 48.96 MHz under no applied load. The total frequency shift is 13.5 MHz with a corresponding membrane displacement of $0.56\ \mu\text{m}$ and a capacitance change of 63 fF, averaging 0.21 MHz/fF. The measured force sensitivity is $26.1\ \text{kHz}/\mu\text{N}$.

1. INTRODUCTION

In a world that a specific user has to be identified for security and safety reasons in operations such as access control and electronic banking, the use of biometric techniques gradually becomes a popular approach for the purpose. The examples include recognition of human speech, iris patterns, and fingerprints. With advances in the semiconductor and MEMS industries, low cost and miniaturization can be achieved simultaneously with integrated tactile sensors. In the past few years, the semiconductor-type tactile sensors have shown great potential to be applied in mobile devices. Most integrated solid-state fingerprint sensors are based on the capacitive sensing mechanisms [1]–[6]. The approach adopted by [1]–[3] requires a minimum or almost no additional micromachining steps. The drawback is that the detection process is sensitive to finger conditions and humidity in the air. The other approach [4]–[6] detects the capacitance change due to the pressure-induced membrane displacement. For a fingerprint sensor implemented as a pixel array, each membrane size is limited to allow a sufficient resolution for recognition of the ridges and valleys on a finger. In this situation, monolithic integration of CMOS sensing circuits with micromechanical structures is necessary in order to promote measured signal-to-noise ratio, which is otherwise negatively impacted by parasitic capacitances in a two-chip solution. The cost for fabrication of CMOS integrated sensors can be high if the micromachining process has to use a whole wafer. As an example, Sato et al. [4] performed

successive deposition and etching steps on a $0.5\ \mu\text{m}$ 3-metal CMOS wafer to realize the pressure-sensing membrane. Different from using a whole wafer process, our approach provides the benefit of a low investment cost, as the required micromachining steps can be performed on a CMOS die. To our best knowledge, no tactile sensor with demonstrated results has been reported by using the same approach. By use of an advanced sub- μm CMOS process, we take advantage of the fast electronics to implement a high-frequency oscillator circuit in order to enhance capacitive sensitivity. From the integration standpoint, the use of a CMOS process with multiple metal layers is beneficial because the proposed fabrication allows the sensing circuit to be placed underneath the pressure-sensing membrane. To our advantage, this approach has a great potential to make a very dense array.

2. DEVICE FABRICATION

The TSMC 0.35 μm two-polysilicon four-metal (2P4M) CMOS process is used for the tactile sensor fabrication. The post micromachining steps are performed on a CMOS die, with no photolithography and film deposition required to form the desired sensing membrane. The process flow in Fig. 1 shows the development of a released membrane structure in cross section. After completion of the CMOS foundry process, the die is mostly covered by the top passivation layer except for the openings beside the membrane. As shown in Fig. 1(b), we perform a sacrificial wet etch of stacked metal and via layers through the openings by using the $\text{H}_2\text{SO}_4/\text{H}_2\text{O}_2$ (2:1) etchant. The solution is constantly heated at 85°C , and H_2O_2 is replenished every 20 minutes to maintain the etching rate. The upper and bottom electrodes for capacitive sensing are formed after sacrificial etch of the metal-3 layer. To avoid stiction due to the remaining liquid in between electrodes, the die is immersed in isopropyl alcohol (IPA) for 30 minutes, followed by a hotplate bake at 90°C for five minutes. The separation between the membrane and the bottom electrode is about $0.64\ \mu\text{m}$ as defined by the metal-3 thickness. The passivation on top of CMOS becomes part of the membrane. These dielectric layers are desired to remain on top of the fabricated tactile sensor for protection and electrical isolation during contact. In Fig. 1(c), we perform a reactive ion etch using the CHF_3/O_2 plasma (100 sccm: 5 sccm) to remove the passivation on top of bond pads, with the sensor area being covered by an overhanging thin tape for etch protection.

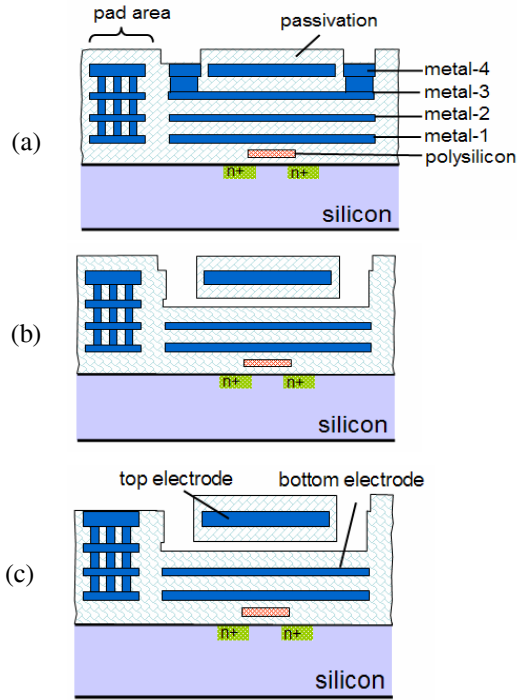


Figure 1: The post CMOS micromachining process.

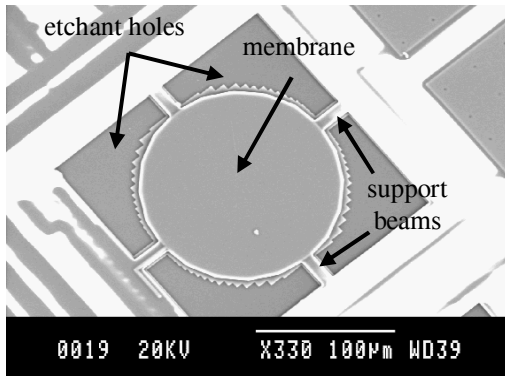


Figure 2: SEM of the fabricated tactile sensor with a radius of $75 \mu\text{m}$. The support beams are $25 \mu\text{m}$ by $10 \mu\text{m}$.

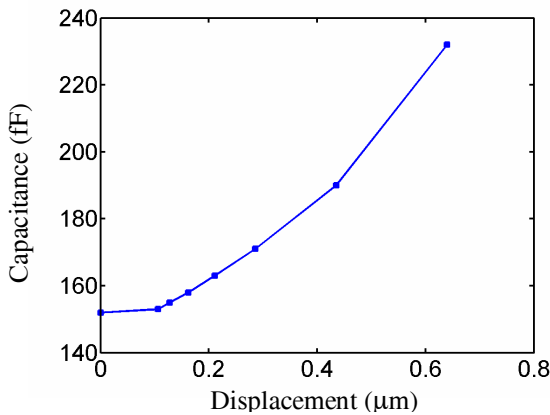


Figure 3: Relationship between the sensing capacitance and the membrane displacement at center.

3. DESIGN

The fabricated pressure-sensing membrane as shown in Fig. 2 consists of multiple dielectric and metal layers. From top to bottom the membrane materials are $\text{Si}_3\text{N}_4/\text{SiO}_2$, aluminum, and SiO_2 , with a total thickness about $3.3 \mu\text{m}$. The membrane of $150 \mu\text{m}$ in diameter is a clamped-clamped structure with four support beams connected to anchors. The metal layer is not placed in the support beams, except for one beam in that a narrow metal-4 line is inserted to connect between the top electrode and the sensing circuit. The support beam consists of the top passivation layer and the dielectric layer between the metal-4 and metal-3. In order to avoid the buckling phenomenon in the out-of-plane direction and to ensure proper structural release, short support beams of $25 \mu\text{m}$ by $10 \mu\text{m}$ are used in the design.

The out-of-plane spring constant of the pressure-sensing membrane is calculated by using the finite-element simulation [8]. The Young's modulus for aluminum, silicon dioxide, and silicon nitride are 70 GPa , 75 GPa , and 210 GPa as used in simulation. The membrane spring constant is obtained as the ratio of the applied pointed force at the membrane center over the associated displacement. The reason for using a concentrated instead of a uniformly distributed load is that the force-displacement relationship is to be verified by a nano-indenter experiment, in which a pointed load is applied by a controlled tip with a radius less than $0.1 \mu\text{m}$. The simulated spring constant is 1876 N/m .

The sensing electrodes are formed by the metal-2 and metal-4 layers in the 2P4M CMOS process. The capacitance consists of an air gap and two dielectric layers on the electrodes, with the latter providing electrical isolation when the top membrane touches the bottom electrode. The initial sensing capacitance is expressed as,

$$C_0 = \frac{\epsilon_0 A}{(h_1 + h_2) \frac{\epsilon_0}{\epsilon_s} + z_0} \quad (1)$$

where ϵ_0 is the permittivity of air, ϵ_s is the permittivity of silicon dioxide, A is the electrode area, h_i is the dielectric thickness, and z_0 is the initial gap separation. Analytically the total sensing capacitance can be obtained by doing a surface integral when knowing the two-dimensional displacement profile of a loaded membrane. Since the representation for the membrane displacement is not available, we resort to finite-element simulations [8] to calculate capacitances under different loads. The relationship of the capacitance with respect to the displacement at center is plotted in Fig. 3, where the capacitance varies from an initial 153 fF to 232 fF for a displacement of $0.64 \mu\text{m}$ as the center touches the bottom.

To detect the capacitance change with respect to the membrane displacement, an astable oscillator [7] as shown schematically in Fig. 4 is used as the sensing circuit, which produces an output frequency shift under an applied load. The ideal waveforms at important nodes are also illustrated in Fig. 4. The circuit as shown consists of four inverters, one resistor, and one capacitor formed by the membrane and the

bottom electrode. The oscillating waveforms are explained as the follows: for $0 \leq t \leq T_1$ when point v_a and v_c are logic high and v_b is logic low, v_a is discharged exponentially from V_{DD} to 0 as expressed by,

$$v_a(t) = V_{DD} e^{-t/RC} \quad (2)$$

The voltage v_a is pulled down to zero immediately after it reaches the threshold voltage V_{th} for logic switch. The time T_1 as shown in Fig. 4 is calculated as,

$$T_1 = RC \cdot \ln\left(\frac{V_{DD}}{V_{th}}\right) \quad (3)$$

Similarly in the next half cycle for $0 \leq t \leq T_2$, v_a rises exponentially from 0 to V_{DD} as expressed by,

$$v_a(t) = V_{DD}(1 - e^{-t/RC}) \quad (4)$$

The time required for v_a to reach V_{th} is T_2 , which is calculated as,

$$T_2 = RC \cdot \ln\left(\frac{V_{DD}}{V_{DD} - V_{th}}\right) \quad (5)$$

The total period is the sum of T_1 and T_2 given by,

$$T = T_1 + T_2 = RC \cdot \ln\left[\frac{V_{DD}^2}{V_{th}(V_{DD} - V_{th})}\right] \quad (6)$$

The value of the polysilicon resistor in Fig. 4 is 30 k Ω . The sensing circuit has a total area of 130 $\mu\text{m} \times 40 \mu\text{m}$, with two power lines and one signal required for routing.

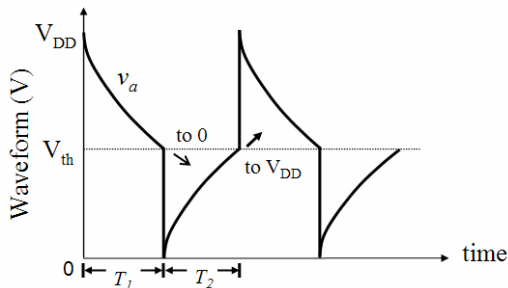
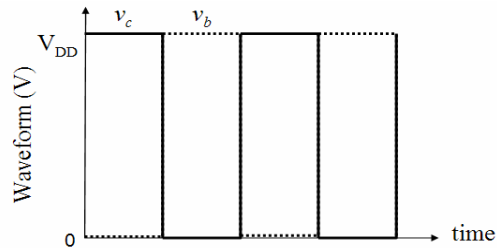
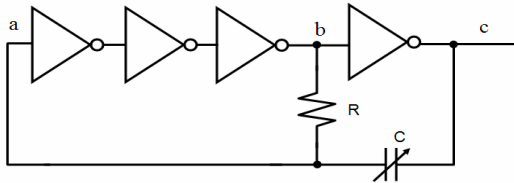


Figure 4: Schematic of the astable circuit with the sensing capacitance C , and the ideal waveforms at points a , b , and c .

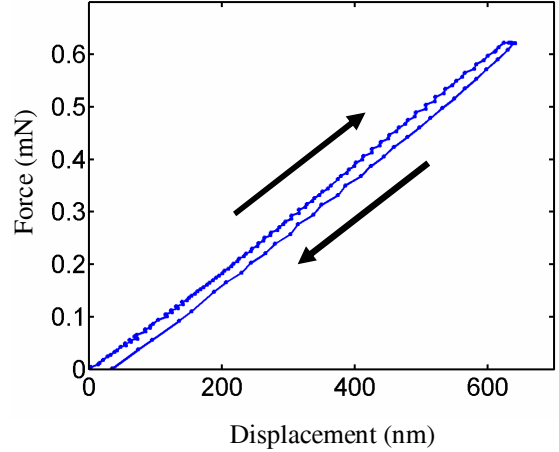


Figure 5: Measured force-displacement curve by a MTS Nanoindenter.

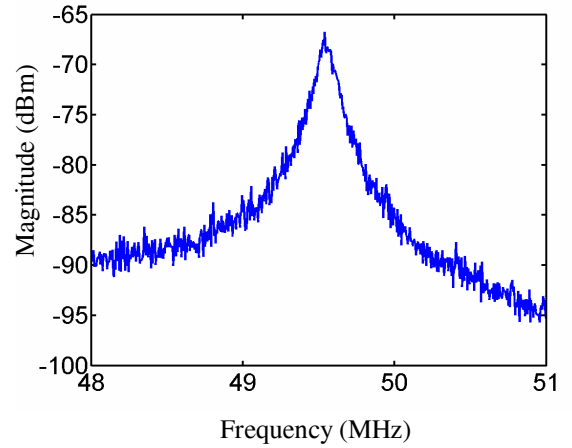


Figure 6: Measured spectral output from the oscillator circuit with no applied load.

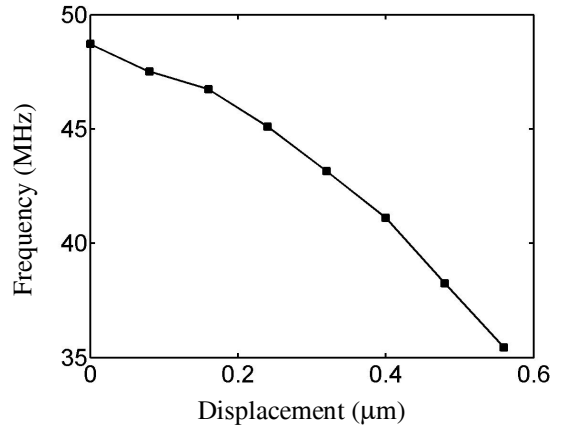


Figure 7: Relationship of the measured frequency with respect to the membrane displacement.

4. EXPERIMENTAL RESULTS

The mechanical characteristic of the released membrane was first measured after the structural release. Its out-of-plane spring constant was measured by using a MTS Nanoindenter, in which a diamond tip was used to apply continuous loading at center of the membrane. The relationship of the force with respect to the associated displacement is shown in Fig. 5, which gives a measured spring constant of 923 N/m. The measured value is smaller than the value from the finite element simulation. The reasons can be attributed to the variation in film thickness, and the film stresses that are not considered in the simulation due to lack of information.

The experimental setup for measuring the circuit output of the released sensor used a sharp tip that was carried and moved by a piezoelectric actuator to give a desired membrane displacement. As shown in Fig. 6, the resonant peak occurs at 48.96 MHz under no applied tip displacement. The membrane was gradually pressed down by the tip, and the output frequency of the oscillator decreased as a result of the increasing sensing capacitance. The relationship of the output frequency with respect to the membrane displacement is plotted in Fig. 7. The total frequency shift is 13.5 MHz with a corresponding displacement of 0.56 μm and a capacitance change from 153 fF to 216 fF. The capacitive sensitivity in terms of the frequency change over the capacitance change is 0.21 MHz/fF. The maximum applied force is 517 μN as calculated by using the product of the measured spring constant and the maximum tip displacement. Thus the sensitivity of the frequency shift with respect to the applied force is 26.1 kHz/ μN .

5. CONCLUSIONS

While most CMOS-micromachined capacitive tactile sensors are known to be fabricated on wafer level, we have demonstrated in this paper a convenient CMOS micromachining process for sensor fabrication on small CMOS dies. The pressure-sensing membrane can be successfully released without stiction as occurred in many wet etching cases. In terms of sensor's performance, the measured sensitivity of 26.1 kHz/ μN is better than most reported data in previous work. The sensor development takes advantages of the multiple metal layers and the fast electronics in a sub- μm CMOS process. The former allows convenient signal routing with the selected membrane and bottom electrode. The latter enhances the sensor performance by producing a high output frequency from the oscillator circuit. Direct integration of the CMOS sensing circuit is important so as to achieve a high oscillation frequency without being affected by parasitic capacitances as in a two-chip solution. The initial output frequency of the sensor with a 153 fF capacitance is measured at 48.96 MHz. As the sensing circuit can be placed directly underneath each sensor, there is a great potential to make a very dense pixel array as a fingerprint sensor by this approach.

ACKNOWLEDGEMENT

This research effort is sponsored by the National Science Council, Taiwan, R.O.C. (NSC 94-2215-E-007-020). The authors would like to thank the National Chip Implementation Center of the National Applied Research Laboratories for support of CMOS fabrication, and Prof. Weileun Fang for use of the laboratory resources.

REFERENCES

- [1] J. W. Lee, D. J. Min, J. Kim, and W. Kim, "A 600-dpi capacitive finger print sensor chip and image-synthesis technique," *IEEE J. Solid-State Circuits*, vol. 34, pp. 469-475, Apr. 1999.
- [2] M. Tartagni and R. Guerrieri, "A fingerprint sensor based on the feedback capacitive sensing scheme," *IEEE J. Solid-State Circuits*, vol. 33, no. 1, pp. 133-142, Jan. 1998.
- [3] K. Machida, S. Shigematsu, H. Morimura, Y. Tanabe, N. Sato, N. Shimoyama, T. Kumazaki, K. Kudou, M. Yano, and H. Kyuragi, "A novel semiconductor capacitive sensor for a single-chip fingerprint sensor/identifier LSI," *IEEE Trans. Electron Devices*, vol. 48, pp. 2273-2278, Oct. 2001.
- [4] N. Sato, K. Machida, H. Morimura, S. Shigematsu, K. Kudou, M. Yano, and H. Kyuragi, "MEMS fingerprint sensor immune to various finger surface conditions," *IEEE Trans. Electron Devices*, vol. 50, no. 4, pp. 1109-1116, Apr. 2003.
- [5] R. J. De Souza and K. D. Wise, "A very high density bulk micromachined capacitive tactile imager," *Int. Conf. on Solid-State Sensors and Actuators (Transducers)*, pp. 1473-1476, Chicago, June 16-19, 1997.
- [6] P. Rey, P. Charvet, M. T. Delaye, and S. Abou Hassan, "A high density capacitive pressure sensor array for fingerprint sensor application," *Int. Conf. on Solid-State Sensors and Actuators (Transducers)*, pp. 1453-1456, Chicago, June 16-19, 1997.
- [7] A. S. Sedra and K. C. Smith, *Microelectronic Circuits*, 5th ed., Oxford University Press, 2004.
- [8] CoventorWare, Coventor, Inc., Cary NC, 2005.